

УДК 539.23: 537.311

V.V.Ivchenko¹, A.N.Sergeev¹, V.S.Elnik¹, and N.M.Chuiko²

Absorption Edge of Cadmium Arsenide

¹*Kherson State University, Chair of Physics, 27, 40 Rokiv Zhovtnya Str., Kherson, 73000, Ukraine,
Phone: +380-0552-326768, E-mail: ivchenko@ksu.kherson.ua*

²*Kherson State Technical University, Department of Cybernetics, 24, Berislavske Shosse, 73008, Kherson, Ukraine,
Phone: +380-0552-516332, E-mail: chuiko@public.kherson.ua*

The experimental data of the Cd₃As₂ absorption edge at low temperature are analyzed for single crystals. The anisotropic Bodnar band model is used to calculate the absorption coefficient. The best fit of the theoretical curve to experimental points is found for the following band parameters: $e_g = -0.1$ eV, $\Delta = 0.33$ eV, $P = 8 \times 10^{-10}$ eV m, $d = 0.12$ eV. The effect of linear in wave vector term in the dispersion equation on the fine structure of the optical absorption spectrum is also discussed.

Keywords: cadmium arsenide, electronic band structure, Bodnar model, dielectric function, optical transitions, spin splitting of bands.

Стаття поступила до редакції 19.05.2003; прийнята до друку 23.10.2003.

I. Introduction

Cadmium arsenide (Cd₃As₂) is a degenerate n-type tetragonal semiconductor of the II-V family with large mobility, low effective mass and highly nonparabolic conduction band [1]. It exhibits an inverted band structure (optical energy gap $e_g < 0$) like HgTe [2] that causes certain interest to this material.

For the adequate description of energy dependent anisotropy of the cyclotron mass and Shubnikov-de Haas (SdH) oscillation period Bodnar [3] proposed band structure model of Cd₃As₂, which satisfied the available experimental data. Despite this fact the results of transport and optical measurements were interpreted within isotropic Kane-type band model [4], [5]. No attempt was made to evaluate independently the values of anisotropic Bodnar model's parameters by analyzing fundamental absorption spectrum.

Some modification (the so-called quasicubic approximation) of Bodnar model was suggested in [6]. In this paper we apply this approach to obtain general expression for interband contribution to the imaginary part of the dielectric function. This expression will be used for the analysis of the experimental data by Gelten *et al.* [5]. Finally, we discuss the influence of linear in wave vector term in the dispersion equation on the fine structure of the Cd₃As₂ absorption edge. Such a term appears as a consequence of symmetry centre lack in this

compound (space group C_{4v}^{12} or I4₁cd) and causes lifting of the twofold spin degeneracy of bands near the Γ point [6]. During last time the effects like these are the object of intensive investigations in two- and three-dimensional systems owing to their potential applications (see *e.g.* [7] and references therein).

II. Theory

The electronic wave function of our problem in the absence of external fields may be written

$$\begin{aligned} \Psi &= \begin{pmatrix} \Psi \uparrow \\ \Psi \downarrow \end{pmatrix} = \\ &= \frac{1}{\sqrt{N}} \exp(ikr) \begin{pmatrix} a_1 S + a_3 Z + a_6 R_- + a_8 R_+ \\ a_2 S + a_4 Z - a_5 R_+ + a_7 R_- \end{pmatrix}, \end{aligned} \quad (1)$$

where N – number of unit cells in crystal, $R_{\pm} = (X \pm iY)/\sqrt{2}$ and the symbols \uparrow and \downarrow mean the spin-up and spin-down functions, respectively. S, X, Y, Z are periodic Bloch amplitudes transformed like atomic s and p functions under the operations of the tetrahedral group at the Γ -point. Coefficients a_i 's satisfy the set of eight algebraic equations, which in the case of quasicubic approximation can be represented in the following matrix form [6]:

$$\begin{pmatrix} \varepsilon_1 & 0 & iK_z + \xi & 0 & 0 & iK_- & 0 & iK_+ \\ 0 & \varepsilon_1 & 0 & iK_z + \xi & -iK_+ & 0 & iK_- & 0 \\ -iK_z + \xi & 0 & \varepsilon_2 & 0 & \Delta_1 & 0 & 0 & 0 \\ 0 & -iK_z + \xi & 0 & \varepsilon_2 & 0 & \Delta_1 & 0 & 0 \\ 0 & iK_- & \Delta_1 & 0 & \varepsilon_3 & 0 & 0 & 0 \\ -iK_+ & 0 & 0 & \Delta_1 & 0 & \varepsilon_3 & 0 & 0 \\ 0 & -iK_+ & 0 & 0 & 0 & 0 & -\varepsilon & 0 \\ -iK_- & 0 & 0 & 0 & 0 & 0 & 0 & -\varepsilon \end{pmatrix} \begin{pmatrix} a_1 \\ a_2 \\ a_3 \\ a_4 \\ a_5 \\ a_6 \\ a_7 \\ a_8 \end{pmatrix} = 0. \quad (2)$$

Here $\varepsilon_1 = \varepsilon_g - \varepsilon$, $\varepsilon_2 = -(\varepsilon + \delta + \Delta/3)$, $\varepsilon_3 = -(\varepsilon + 2\Delta/3)$, $\Delta_1 = \sqrt{2}\eta\Delta/3$, $K_z = \eta^2 P k_z$, $K_{\pm} = (\mp iP/\sqrt{2})(k_x \pm ik_y)$, where k_x, k_y, k_z are components of the wave vector \mathbf{k} and zero of energy ε is chosen at the top of the heavy-hole valence band. Therefore the model along with ε_g needs to know the values of Kane's [8] spin-orbit splitting of valence band Δ and interband momentum matrix element P , "crystal

field" parameters δ and ξ [9], [6], index of the tetragonal distortion of lattice η [10] (for 4mm crystal class $\eta = c/2a$, where a, c are lattice constants).

Let us express $a_3 \dots a_8$ in terms of a_1, a_2 and eliminate them by substituting in the first two equations of set (2). Then proceeding to the spherical coordinate system we obtain

$$\begin{pmatrix} \gamma - (f_1 \sin^2 \theta + f_2 \cos^2 \theta)k^2 & -2i(f_3 e^{-i\theta} \sin \theta)k \\ 2i(f_3 e^{i\theta} \sin \theta)k & \gamma - (f_1 \sin^2 \theta + f_2 \cos^2 \theta)k^2 \end{pmatrix} \begin{pmatrix} a_1 \\ a_2 \end{pmatrix} = 0, \quad (3)$$

where γ, f_i – polynomials concerning band parameters and energy. Their extended forms are given in [6]. Setting the determinant of matrix in (3) equal to zero gives the following equation for finding energy spectrum:

$$\gamma = (f_1 \sin^2 \theta + f_2 \cos^2 \theta) k^2 + 2\sigma(f_3 \sin \theta)k, \quad \sigma = \pm 1. \quad (4)$$

Equations (3) together with the eigenvalue equation (4) lead to an algebraic relation between a_1 and a_2 :

$$a_2 = -i\sigma e^{i\theta} a_1. \quad (5)$$

Using this relation one may express the rest of the

coefficients $a_3 \dots a_8$ by a_1 , which can be found in its turn from the normalization condition: $\sum_i |a_i|^2 = 1$. So, the whole wave function (1) is in principle determined. We do not give here the expression for it on account of its complexity.

The resulted from equation (4) anisotropic energy band scheme of Cd_3As_2 is qualitatively depicted in Fig. 1. At $\theta = 0$ equation (4) describes four twofold degenerate bands: conduction (c) band, which has at

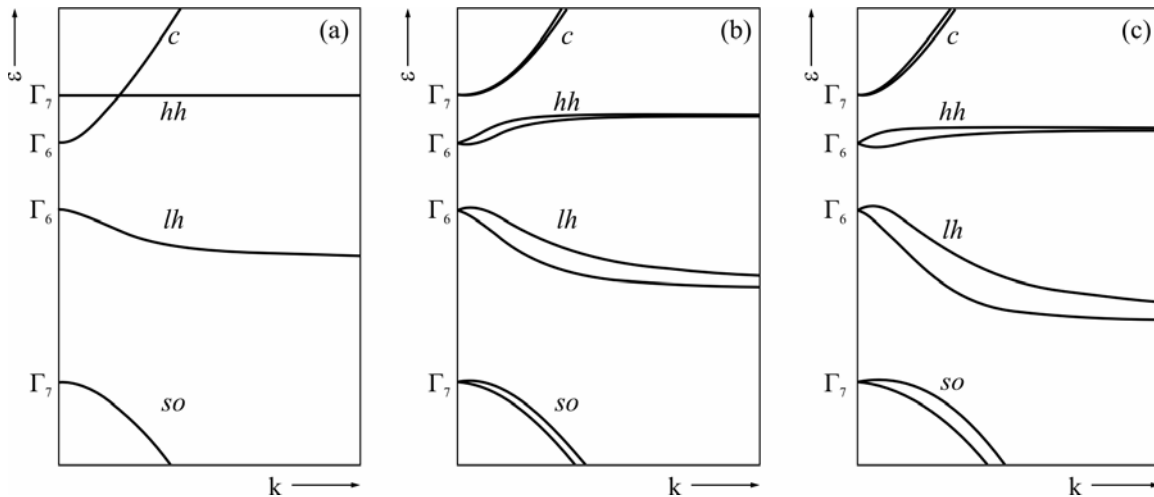


Fig. 1. Structure of Cd_3As_2 conduction and valence bands near $\mathbf{k} = 0$ (schematically). The wave vector makes an angle with tetragonal c -axes of $\theta = 0$ (a), $\theta = \pi/4$ (b) and $\theta = \pi/2$ (c), respectively.

$\mathbf{k} = 0$ symmetry Γ_7 ; Γ_6 heavy-hole (*hh*) valence band, split from Γ_8 due to the tetragonal field splitting; Γ_6 light-hole (*lh*) valence band and Γ_6 spin-orbit split-off (*so*) valence band. The flat parts of the conduction and heavy-hole band are a consequence of neglecting higher energy levels as well as free-electron term, which will give finite curvature of the bands at this angle. Fig. 1 also indicates that these bands come into contact only at one (with $\theta = 0$ and arbitrary polar angle φ) \mathbf{k} value and the energy gap becomes zero at this point. Similar situation takes place in cubic zero-gap semiconductors but there such a degeneration of bands exists at $\mathbf{k} = 0$. The finite value of \mathbf{k} for Cd_3As_2 is caused by the positive sign of δ parameter [10].

Due to the difference between f_1 and f_2 the shape of the dispersion curves changes when changing the direction of the wave vector. Moreover, at $(\theta, \mathbf{k}) \neq 0$ the double degeneracy of all four bands is removed by term proportional to $\mathbf{k} \sin \theta$. As a result of this splitting

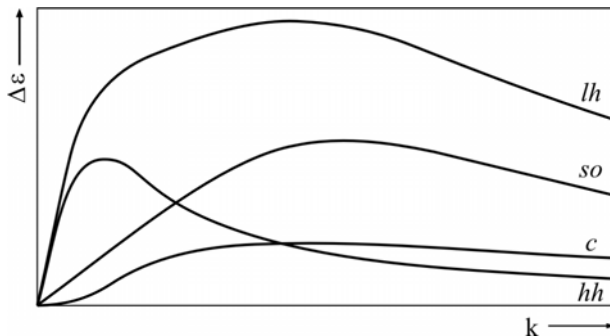


Fig. 2. Spin splitting of the subbands as a function of wave number for $\theta = \pi/2$ (schematically).

where ϵ_0 – dielectric constant, and $j = 1, 2$ is index of appropriate valence band. The other designations have the same sense as in [11]. Taking into account Burstein-Moss shift, which always exists in degenerate semiconductors, it is necessary to insert into the integrals of equation (6) in analogy with [12] factor

$$\epsilon_2(\omega) = \frac{e^2}{6\pi\epsilon_0} \sum_{j, y_c, y_j} \int_0^{p/2} \sin \theta d\theta \int_0^\infty k^2 dk \int_0^{2\pi} \left| \langle \mathbf{U}_c^c | \mathbf{e}_\theta | \mathbf{U}_j^j \rangle \right|^2 \delta(\epsilon_c^{y_c} - \epsilon_j^{y_j} - \hbar\omega) d\varphi, \quad (6)$$

The integration over θ in the case of highly nonparabolic bands may be performed analytically only in cubic approximation ($\delta = \xi = 0$, $\eta = 1$) that leads to

minimum of the heavy-hole band and maximum of the light-hole and split-off bands are shifted from $\mathbf{k} = 0$ on the so-called “loops of extrema” (circles with appropriate radius, lying in the $k_x k_y$ plane) [6], whereas minimum of the conduction band is located at the Γ -point. The divergence of the subbands, which differ in signs of index σ in equation (4), reaches maximum at $\theta = \pi/2$. From Fig. 2 it is visible that the largest divergence exists between the subbands of the light-hole band.

Now we are going to derive the expression for interband contribution to the optical absorption within the framework of the presented band structure model. Because Cd_3As_2 is an n-type degenerate material (the Fermi level is high in the conduction band) only transitions from the heavy-hole and light-hole valence bands to conduction band are possible in the spectral region of interest. Adopted for our problem the well-known formula for the imaginary part of the dielectric function produced by direct transitions [11] is given by

$$f_j^{y_c, y_j} = f(\epsilon_j^{y_j}) - f(\epsilon_c^{y_c}), \quad (7)$$

where $f(\epsilon_j^{y_j})$, $f(\epsilon_c^{y_c})$ denote the Fermi-Dirac distribution functions of the participating subbands. The next step is to calculate the transition probability $\left| \langle \mathbf{U}_c^c | \mathbf{e}_\theta | \mathbf{U}_j^j \rangle \right|^2$. Since the wave functions (1) are already known one may obtain for unpolarized light (unfortunately, up to now there is no available data as for the polarization dependence of fundamental absorption edge of Cd_3As_2):

$$\left| \langle \mathbf{U}_c^c | \mathbf{e}_\theta | \mathbf{U}_j^j \rangle \right|^2 = \frac{m^2 P^2}{3\hbar^2} M_j^{y_c, y_j}, \quad (8)$$

where the expression for $M_j^{y_c, y_j}$ is given in the Appendix. Using axial symmetry of problem, properties of δ -function, and equations (7), (8) it is possible to reduce equation (6) to

widely used Kane's result [8]. The only way to consider partially the tetragonal symmetry of crystal was proposed by Pawlikowsky *et al.* [13], [14] while calculating the

absorption spectra of isomorphous compounds Zn_3P_2 and Zn_3As_2 . In these works the effect of “crystal field” interaction on the energy levels arrangement at the Γ point was taken into account but bands nevertheless were considered as isotropic. Such a procedure is not valid for Cd_3As_2 at least because its heavy-hole band has not standard Kane-type form with maximum at $\mathbf{k} = 0$. It happens, however, that modern computer capacity enables to calculate the integrals in (9) numerically without any simplifications during rather short time term.

III. Numerical fit

In order to reveal the characteristic features of the presented energy spectrum it is necessary to investigate absorption edge at low temperature. The reason is that with increasing of the latter the Fermi-step is washing out and all the singularities of the absorption curve disappear. So, we have chosen the experimental data by Gelten *et al.* [5], who performed optical measurements on thin crystalline samples, which were mounted very carefully without mechanical strains at low temperatures. Fig. 3 shows the absorption coefficient α versus wavelength at 10 K in a sample with an electron concentration of $1.0 \times 10^{24} \text{ m}^{-3}$ that has been lapped and etched to a thickness of 11 μm . To compare this spectrum with theoretical dependences

$$\alpha(\omega) = \frac{\omega}{c} \sqrt{2(\sqrt{\epsilon_2^2 + \epsilon_1^2} - \epsilon_1)} \quad (10)$$

the real part $\epsilon_1(\omega)$ of the dielectric function was calculated beforehand by Kramers-Kronig relations from

the imaginary part $\epsilon_2(\omega)$ and the high-frequency dielectric constant $\epsilon_\infty = 16$ [5] was chosen. There is of course the free carrier contribution in equation (10), which plays dominant role in the long-wavelength range at high temperatures. However, at low temperatures near the absorption edge it becomes too small and may be neglected.

The most reliable values of band parameters $\epsilon_g = -0.095 \text{ eV}$, $\Delta = 0.27 \text{ eV}$, $P = 7.4 \times 10^{-10} \text{ eV m}$ (P_\perp in notation by Bodnar), $\delta = 0.095 \text{ eV}$ were estimated by Blom *et al.* [3] from SdH measurements. The value of $\eta = 1.004695$ was determined directly from x-ray analysis [15]. There is no experimental data as to the value of the parameter ξ . This quantity vanishes in materials with inversion symmetry. Hence it seems reasonable to neglect it in the first approximation, because in general the effects caused by inversion asymmetry are small. It will be restored while discussing the influence of spin splitting of bands on the fine structure of the absorption spectrum.

Using the above-mentioned set of parameters as the initial we have generated a large number of theoretical curves by varying the values of ϵ_g , Δ , P , δ and Fermi energy ϵ_F . The best fit to the experimental points was obtained for the parameters listed in Table 1, and is shown in Fig. 3.

IV. Discussion

To explain the stepped behavior of the absorption

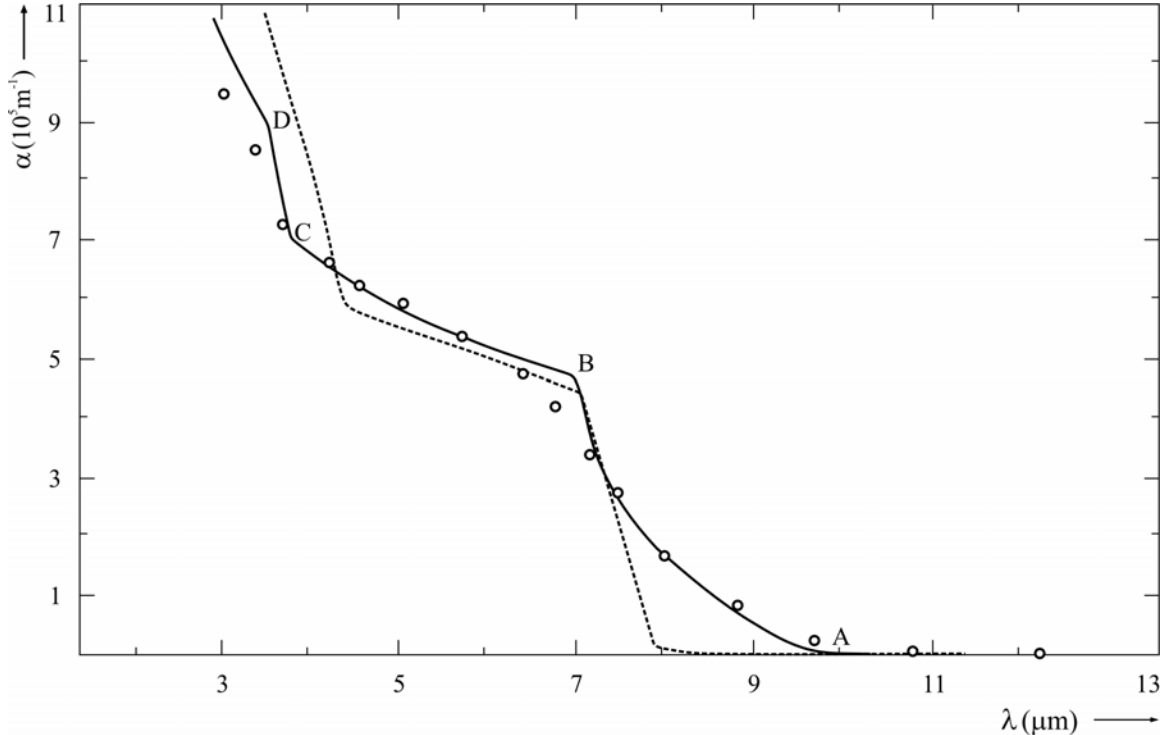


Fig. 3. Optical absorption coefficient of Cd_3As_2 at 10 K. Dashed line: the best fit within Kane model with a modified isotropic heavy-hole band [5]; solid line: the best fit within Bodnar model. Points show experimental values as measured by Gelten *et al.* [5]. The electron concentration of the sample at 300 K is $1.0 \times 10^{24} \text{ m}^{-3}$

Table 1.Energy band parameters of Cd₃As₂.

Parameter	ε_g	Δ	P	δ
Value	-0.1 eV	0.33 eV	8×10^{-10} eV m	0.12 eV

coefficient at low temperature Gelten *et al.* used the isotropic inverted Kane model. In this model two distinct steps on the absorption curve (dashed line in Fig. 3) correspond to direct transitions from the heavy-hole and light-hole bands to the conduction band. Steps of this kind in the infrared region were previously observed by Szuskiewicz on HgSe [16] and HgTe [17]. Our fitting curve (solid line in Fig. 3) also indicates the existence of these steps. Moreover, comparing both theoretical curves with experimental data one can conclude that in the anisotropic model the structure of steps is more corresponding to reality. Let us consider this circumstance in detail. At absolute zero temperature transitions from the heavy-hole band to the conduction one begin at the photon energy equal to ε_F . However, due to the anisotropy of bands these transitions are possible only between states with $\theta = 0$. The transitions between states with $\theta = \pi/2$ appear for some greater photon energy. So, according to equation (9) in this spectral region (interval AB in Fig. 3) the absorption coefficient increases rapidly unlike isotropic model within which this quantity unevenly changes at the photon energy equal to ε_F . The same effect occurs on the interval CD where transitions from the light-hole band appear. There will be additional washing out of steps caused by long-range potential fluctuations and by washing out of the Fermi-step. However, for low temperatures the considered mechanism should be predominant. There is no such an effect for anisotropic nondegenerate semiconductors in which interband transitions with all θ appear for the same photon energy equal to ε_g .

In order to improve agreement with the experiment Gelten *et al.* introduced a phenomenological $\varepsilon(\mathbf{k})$ relation for the heavy-hole band resulting in its maximum shifted from the Γ point [5]. The quoted authors pointed out that this modification could be considered as a directional average of the valence band energies in Bodnar model like the spherical approximation for the warping terms [17]. Such a procedure of averaging quite correctly reproduces the influence of the small warping terms but in our case it turns to be an oversimplification. In fact, the shift of the heavy-hole band maximum leads to the shift of the threshold of the first step (point B) but not to washing out of this step.

It should be emphasized that within Bodnar model the width of intervals AB and CD is very sensitive to the value of crystal-field splitting parameter δ and tends to zero if $\delta \rightarrow 0$. The value of δ estimated here, is close to that obtained by Chuiko [18], $\delta = 0.11$ eV, from analysis of SdH data for a sample with the most pronounced

anisotropy (the electron concentration at 4.2 K was $1.2 \times 10^{23} \text{ m}^{-3}$).

Similar to HgSe [16] in our calculations the threshold of the second step strongly depends on the values of ε_g and Δ and increases when these values increase. The difference between Blom's estimation for Δ and that proposed by us probably comes from the fact that this parameter has greater influence on the curvature of the light-hole band than on the conduction one. On the other hand SdH measurements give direct information about the shape of the conduction band only. The value of Δ estimated here coincides with that proposed by Cisowski [19].

Parameter P affects only the magnitudes of the absorption coefficients, which decrease when the value of P increases. The reason is that with increasing of P the joint density of states decreases faster than the transition probability increases. Regarding some overstated P value in comparison with those reported in literature [3] one may object that the higher band corrections to the both wave functions and joint density of states were not taken into account in our calculations. If this corrections are done the values of the absorption coefficients have to be smaller [17], and overstating of P is not necessary. The deviation of the theoretical curve from the experimental points in the region of the second step is probably also caused by neglecting the second order perturbation theory. This theory however is going to be very complicated for Cd₃As₂ because involves many more parameters than for the cubic crystals [3].

Consider now the effect of bands spin splitting on the fine structure of the absorption edge. For nondegenerate semiconductors that is the case (see Boiko [20]). Hopfield [21] analyzed the influence of such a splitting on the exciton spectra of wurtzite CdS. Within the framework of the presented model the value of each band splitting depends on the value of parameter ξ , which is defined by "interaction" between S and Z states via asymmetric part of the crystal potential. In principle, the value of ξ could be estimated from the analysis of beating patterns in the quantum oscillations [22] like in zinc-blende crystals [23-25]. Unfortunately, there were no purposive investigations of this effect in Cd₃As₂. If we identify ξ with activation energy of phase transition that is accompanied by symmetry centre lack in this compound, then we get $\xi_{\max} = 0.035$ eV as an upper limit of this quantity. Using parameters listed in Table 1 ξ can be varied in range $0 \leq \xi \leq \xi_{\max}$ to see the effect of bands splitting on the absorption. The results of this variation are represented in Fig. 4 in form of the derivative of the absorption coefficient near the

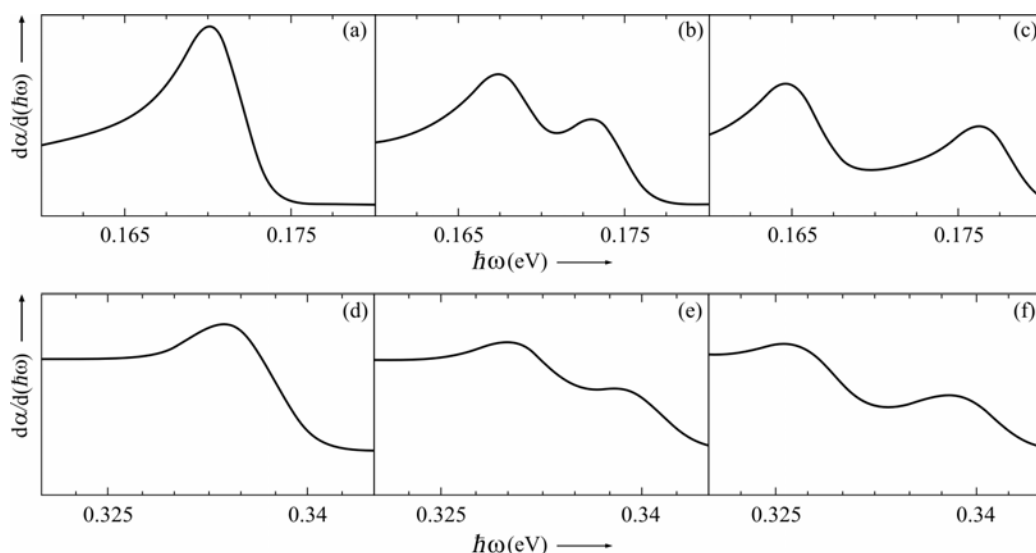


Fig. 4. Theoretical effect of increased spin splitting on the modulated absorption spectrum near fractures B (a-c) and D (d-f) on the integral curve. (a) and (d) $\xi = 0$; (b) $\xi = 15$ meV; (c) $\xi = 30$ meV; (e) $\xi = 5$ meV; (f) $\xi = 8$ meV. The electron concentration and temperature of the sample are the same as in Fig. 3.

appearing singularities. At $\xi = 0$ one can see two peaks, which correspond to the fractures B and D on the integral curve. If $\xi \neq 0$ both peaks are split as a consequence of the fact that transitions from two subbands of the heavy-hole or light-hole band appear at $\theta = \pi/2$ for slightly different photon energies. It is important that the distance between positions of peaks in each doublet is equal to energy splitting of the appropriate valence band at $k_F(\pi/2)$. Since splitting of the light-hole band is larger than of the heavy-hole one, peaks, corresponding to the fracture B, can be resolved for smaller values of ξ (Fig. 4e,f). Therefore, we conclude that the experimental investigation of these singularities in modulated absorption spectra should provide the most direct way for determining the value of ξ .

ACKNOWLEDGEMENTS

We are grateful to Dr. M. J. Gelten for graciously providing his experimental data. We also wish to thank Dr. G.P. Chuiko for estimation of activation energy, and Dr. I.E. Maronchuk for critical reading of the manuscript.

В.В. Івченко – магістр фізики, асистент кафедри фізики;
В.С. Єльнік – магістр фізики, лаборант кафедри фізики;
О.М. Сергєєв – магістр фізики, лаборант кафедри фізики;
Н.М. Чуйко – кандидат фізико-математичних наук, доцент кафедри вищої математики.

- [1] K.Sieranski, J.Szatkowski, J.Misiewicz. Semiempirical tight-binding band structure of II_3V_2 semiconductors: Cd_3P_2 , Zn_3P_2 , Cd_3As_2 , and Zn_3As_2 // *Phys. Rev.*, **B50**(11), pp.7331-7337 (1994).
- [2] E.K.Arushanov. Crystal Growth & Characterization of II-V Compounds // *Progr. Cryst. Growth & Charact.*, **25**, pp.131-201 (1992).
- [3] F.A.P.Blom. Electronic properties of Cd_3As_2 // *Lectures Notes in Physics*, **133**, pp.191-211 (1980).
- [4] F.A.P.Blom, M.J.Gelten. Temperature dependence of electron concentration in cadmium arsenide // *Phys. Rev.*, **B19**(4), pp.2411-2413 (1979).
- [5] M.J.Gelten, C.M. van Es, F.A.P.Blom and J.W.F.Jonganeelen. Optical verification of the valence band structures of cadmium arsenide // *Solid State Commun.*, **33**, pp.833-836 (1980).
- [6] G.Chuiko, N.Don, O.Dvornik, V.Ivchenko, A.Sergeev. Simple inverted band structure model for cadmium arsenide (Cd_3As_2) // *Moldavian Journal of the Physical Sciences*, **2**(1), pp.88-94 (2003).
- [7] Z.Wilamowski, W.Jantsh. ESR studies of the Bychkov-Rashba field in modulation doped Si/SiGe quantum wells // *Physica E*, **20**, pp.439-442 (2002).
- [8] E.O.Kane. Band structure of Indium Antimonide // *Journ.Phys.Chem.Solids*, **1**, pp.249-261 (1957).
- [9] H.Kildal. Band structure of CdGeAs_2 near $\mathbf{k} = 0$. // *Phys. Rev.*, **B10**(12), pp.5082-5087 (1974).
- [10] Г.П.Чуйко, О.В.Дворник. Зв'язок між кристалічним розщепленням валентних зон та тетрагональною деформацією ґратки для сполук II_3V_2 // *Фізика і хімія твердого тіла*, **3**(4), с.682-686, (2002).
- [11] Ф. Бассани и Дж. Пастори Парравичини. *Электронные состояния и оптические переходы в твердых телах*. Наука, М. 392 с. (1982).

- [12] M.J.Gelten, A. van Lieshout, C. van Es, F.A.P.Blom. Optical properties of Cd₃P₂ // *J. Phys. C*, **11**, pp.227-237 (1978).
- [13] J.M.Pawlikowski. Absorption edge of Zn₃P₂ // *Phys. Rev.* **B26**(8) pp. 4711-4713 (1982).
- [14] B.Sujak-Cyruł, B.Kolodka, J.Misiewicz, J.M.Pawlikowski. Intraband and interband optical transitions in Zn₃As₂. // *Journ.Phys.Chem.Solids*, **1**, pp.249-261 (1957).
- [15] G.A.Steingman, J.Goodycar. The crystal structure of Cd₃As₂ // *Acta. Crystallogr.* **B24**, pp.1062-1067 (1968).
- [16] W.Szuskiewicz. Interband absorption and the Γ point band structure parameters in HgSe // *Phys. Stat. Sol.* **B91**, pp.361-369 (1979).
- [17] W.Szuskiewicz. Optical absorption in HgTe // *Phys. Stat. Sol.* **B79**, pp.691-698 (1977).
- [18] Чуйко Г.П. Структура дна зоны проводимости арсенида кадмия // *ФТП*, **16**(5), с. 609, (1982) (аннотация).
- [19] J.Cisowski. Level ordering in III₂V₂ semiconducting compounds // *Phys. Stat. Sol.* **B111**, pp.289-293 (1982).
- [20] И.И.Бойко. Оптические свойства полупроводников с петлей экстремумов. // *ФТП*, **3**(7), с.1950-1953 (1961).
- [21] G.D.Mahan, J.J.Hopfield. Optical effects of energy terms linear in wave vector. // *Phys. Rev* **135**, pp.A428-A433 (1964).
- [22] M.J.Aubin, J.C.Portal. Shubnikov-de Haas oscillations in Cd_{3-x}Zn_xAs₂ // *Solid State Commun.*, **38**, pp.695-402 (1981).
- [23] D.G.Seiler and W.M.Becker and L.M.Roth. Inversion-asymmetry splitting of the conduction band in GaSb from Shubnikov-de Haas measurements. // *Phys. Rev* **B1**(2), pp.764-775 (1970).
- [24] D.G.Seiler, B.D.Bajaj, and A.E.Stephens. Inversion-asymmetry splitting of the conduction band in InSb. // *Phys. Rev* **B16**(6), pp.2822-2833 (1977).
- [25] M.M.Miller and R.Reifenberger. Magnetic breakdown and de Haas-van Alphen effect in Hg_{1-x}Fe_xSe. // *Phys. Rev* **B38**(5), pp.3423-3432 (1988).

APPENDIX

The quantity $M_j^{y_c, y_j}$ that appears in equation (8) for $\sigma_c \sigma_j = 1$ is given by

$$M_j^{y_c, y_j} = |a_c^{y_c}|^2 |a_j^{y_j}|^2 \left[(\bar{\sigma}_1^+ P k \sin \eta - \bar{\sigma}_2^+ y_c \xi)^2 + (\bar{\sigma}_2^- P k \sin \eta + \bar{\sigma}_3^- y_c \xi)^2 + ((\bar{\sigma}_2^-)^2 + (\bar{\sigma}_3^+)^2) \eta^4 P^2 k^2 \cos^2 \eta \right] \quad (\text{A } 1)$$

For $\sigma_c \sigma_j = -1$

$$M_j^{y_c, y_j} = |a_c^{y_c}|^2 |a_j^{y_j}|^2 \left[(\bar{\sigma}_1^- P k \sin \eta - \bar{\sigma}_2^+ y_c \xi)^2 + (\bar{\sigma}_2^-)^2 z^4 P^2 k^2 \cos^2 \eta \right] \quad (\text{A } 2)$$

In these expressions

$$|a|^{-2} = \left[\frac{1 + \frac{P^2 k^2 \sin^2 \eta}{2e^2} + \frac{\frac{1}{2} \left(\left(e + d + \frac{D}{3} \right) P k \sin \eta + \frac{2z D y_c \xi}{3} \right)^2 + \left(\left(e + \frac{2D}{3} \right)^2 + \frac{2z^2 D^2}{9} \right) z^4 P^2 k^2 \cos^2 \eta}{\left(\left(e + \frac{2}{3} D \right) \left(e + d + \frac{1}{3} D \right) - \frac{2}{9} z^2 D^2 \right)^2} + \frac{\left(\frac{z D P k \sin \eta}{3} + y_c \left(e + \frac{2D}{3} \right) \right)^2}{\left(\left(e + \frac{2}{3} D \right) \left(e + d + \frac{1}{3} D \right) - \frac{2}{9} z^2 D^2 \right)^2} \right]^{-1} \quad (\text{A } 3)$$

$$\bar{\sigma}_1^\pm = -\frac{1}{2} \left[\frac{\left(\frac{e_c^{y_c} + d + D/3}{\left(e_c^{y_c} + \frac{2}{3} D \right) \left(e_c^{y_c} + d + \frac{1}{3} D \right) - \frac{2}{9} \eta^2 D^2} \right)^\pm}{\left(\frac{e_j^{y_j} + d + D/3}{\left(e_j^{y_j} + \frac{2}{3} D \right) \left(e_j^{y_j} + d + \frac{1}{3} D \right) - \frac{2}{9} \eta^2 D^2} \right)} + \left(\frac{1}{e_j^{y_j}} \pm \frac{1}{e_c^{y_c}} \right) \right] \quad (\text{A } 4)$$

$$\sigma_2^\pm = \frac{3D}{3} \left(\frac{1}{\left(e_j^{y_j} + \frac{2}{3}D \right) \left(e_j^{y_j} + d + \frac{1}{3}D \right) - \frac{2}{9}3^2D^2} \pm \frac{1}{\left(e_c^{y_c} + \frac{2}{3}D \right) \left(e_c^{y_c} + d + \frac{1}{3}D \right) - \frac{2}{9}3^2D^2} \right) \quad (\text{A } 5)$$

$$\sigma_3^\pm = \left(\frac{e_j^{y_j} + 2D/3}{\left(e_j^{y_j} + \frac{2}{3}D \right) \left(e_j^{y_j} + d + \frac{1}{3}D \right) - \frac{2}{9}3^2D^2} \pm \frac{e_c^{y_c} + 2D/3}{\left(e_c^{y_c} + \frac{2}{3}D \right) \left(e_c^{y_c} + d + \frac{1}{3}D \right) - \frac{2}{9}3^2D^2} \right) \quad (\text{A } 6)$$

В.В.Івченко¹, О.М.Сергеев¹, В.С. Єльнік¹, і Н.М.Чуйко²

Край поглинання арсеніда кадмія

¹Херсонський Державний університет, кафедра фізики, 40 років Жовтня 27, Херсон, 73000, Україна, тел. +380-0552-326768, e-mail: ivchenko@ksu.kherson.ua

²Херсонський державний технічний університет, факультет кібернетики, лабораторія теорії твердого тіла, Бериславське шосе, 24, 73008, Херсон, Україна, тел. +380-0552-516332, e-mail: chuiiko@public.kherson.ua

Аналізуються експериментальні дані стосовно краю поглинання кристалічного Cd₃As₂, отримані при температурі 10К. Обчислення коефіцієнта поглинання вперше проведено у межах анізотропної зонної моделі Боднара. Найкращий збіг теоретичної кривої з експериментальними точками одержано для наступних зонних параметрів: $e_g = -0.1$ еВ, $\Delta = 0.33$ еВ, $P = 8 \times 10^{-10}$ еВ м, $d = 0.12$ еВ. Обговорюється також вплив лінійного по хвильовому вектору доданка в дисперсійному рівнянні на тонку структуру оптичного спектра поглинання.